PRAMANA
— journal of
physics

Vol. 55, Nos 1 & 2
July & August 2000
pp. 85–100

Quantum chromodynamics studies at LEP2

SUNANDA BANERJEE
Tata Institute of Fundamental Research, Homi Bhabha Road, Mumbai 400 005, India

Abstract. Several studies have been made to the hadronic final states in e^+e^- collisions at LEP. Studies of the annihilation process at LEP2 have given rise to results on jet rate, event shape, heavy flavour production, inclusive momentum spectra, Bose–Einstein correlation and colour reconnection effects. Event shape studies have given rise to accurate determination of the strong coupling constant α_s using $\mathcal{O}\left(\alpha_s^2\right)$ with resummed leading and next-to-leading log calculation and also with power law corrections. Studies of 2-photon processes have yielded results on $\gamma\gamma$ cross-section, heavy flavour production, photon structure function and $\gamma^\star\gamma^\star$ scattering.

Keywords. Quantum chromodynamics; large electron positron collider.

PACS Nos 12.20.-m; 12.38.Qk; 13.65.+i

1. Introduction

The four experiments, ALEPH, DELPHI, L3 and OPAL, operating at the large electron positron collider (LEP) took data at centre of mass energies around m_Z during 1989–1995. Since then, LEP has been operating at energies above the threshold of W^+W^- production. At these energies, 2-photon reactions and hadron production through annihilation are the two most dominant processes. So, these processes will have low background and high statistics and they can be studied with small systematic error.

On the other hand, these processes will be background to new particle searches and W/Z pair production studies. One requires a thorough understanding of QCD backgrounds to make meaningful searches of new phenomena.

Production processes are well defined in these studies. There is hadronic activity only in the final state. Also, the effect of hadronization decreases with increasing centre of mass energies. This implies that jets will retain initial parton direction. So the hadronic data at LEP2 will allow clean test of QCD with minimum assumptions.

2. Annihilation process

There are three sources of data for these studies:

- Data at reduced $\sqrt{s'}$ from hadronic Z decays with an energetic isolated photon (of energy E_γ) with typical sample size of a few 1000 events.

$$\sqrt{s'} = \sqrt{s\left(1 - 2\frac{E_\gamma}{\sqrt{s}}\right)}.$$

L3 has measurements in 6 energy bins between 30–86 GeV whereas DELPHI has measurements in 3 energy bins between 32–80 GeV. The dominant background for these events are due to π^0/η^0 decays.

- Data from hadronic Z decays at $\sqrt{s} \approx m_Z$ where sample size of few 100 K events exists for each of the four experiments, ALEPH, DELPHI, L3, OPAL. Background is negligible for these samples.
- High energy data at $\sqrt{s}$ = 130, 136, 161, 172, 183, 189, 192–202 GeV coming from ALEPH, DELPHI, L3, OPAL experiments. The high energy data samples vary from a few 100's to a few 1000's depending on $\sqrt{s}$. These data have substantial backgrounds due to ISR γ (radiative return to Z) and due to W^+W^-, ZZ production.

2.1 *Jet rate*

Jets have been reconstructed with different jet algorithms as a function of jet resolution parameter. Figure 1 shows a comparison of the jet rate for Cambridge algorithm obtained by the DELPHI collaboration [1] at $\sqrt{s}$ = 189 GeV as a function of the jet resolution parameter with predictions from various parton shower Monte Carlo programs. Jet rates as a function of $y_{\rm cut}$ are well described by the parton shower approach.

JADE data have been re-analysed [2] in view of improved theoretical understandings. JADE and OPAL data are now presented in a coherent approach for jet rate studies. Jet rates as a function of centre of mass energy have been fitted using evolution of α_s ala QCD with the scale fixed at 1 or kept as a parameter in the fit. The optimized

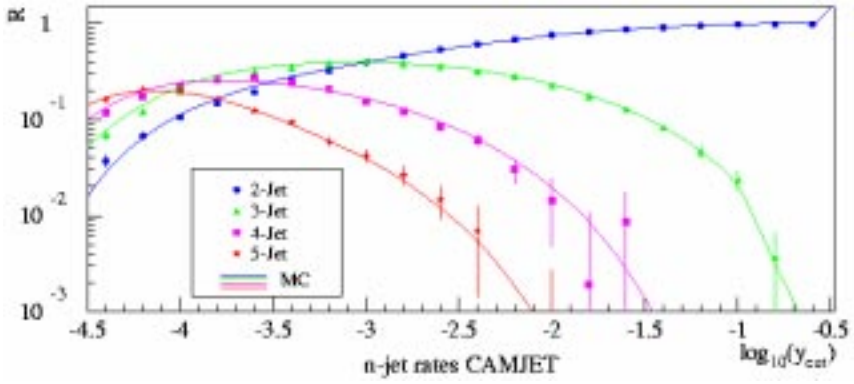

Figure 1. Jet rate as measured by DELPHI at $\sqrt{s}$ = 189 GeV using the Cambridge algorithm as a function of jet resolution parameter.

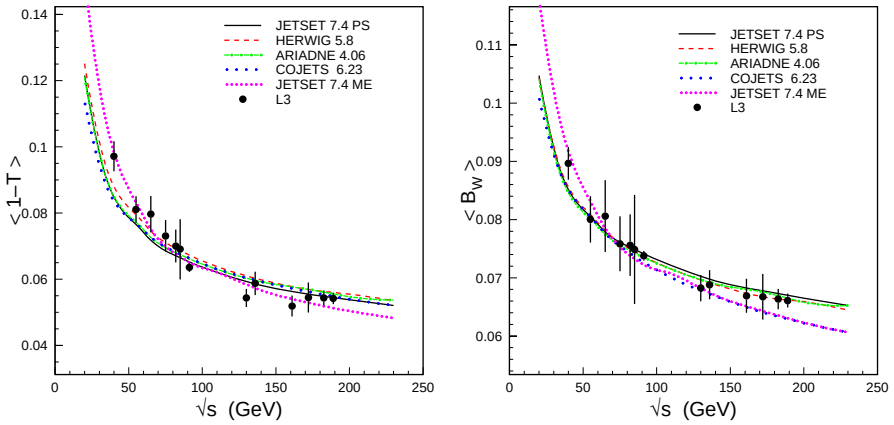

Figure 2. Energy evolution of the mean event shape variables, $1-T$, B_W as measured by L3 compared with different QCD model predictions

scale does not improve fit quality. So from a study of jet rates, OPAL quote an $\alpha_s(m_Z)$ value of $0.1181^{+0.0066}_{-0.0056}$.

2.2 *Event shape*

Several event shape variables have been studied to examine the hadronic event structure in the high energy e^+e^- data. The variables, event thrust, scaled heavy jet mass, C-parameter, have been used to describe the longitudinal shower development. On the other hand, the two jet broadening variables (total and wide) are used to describe the transverse shower development. All these variables are sensitive to hard gluon emission describing multi-jet topology.

To make these studies, hadronic events are selected using their characteristic properties: large visible energy, high multiplicity, etc. To obtain small systematic errors, backgrounds due to 2-photon, ISR, W^+W^-/ZZ are actively rejected. The distributions are then corrected for detector effects: resolution, acceptance, $\cdots$ using simulated data from parton shower Monte Carlo programs.

The corrected distributions can be compared to different QCD models tuned with data at LEP1. The models used by the LEP experiments comprise (1) JETSET using coherent parton shower for the perturbative QCD part and a string fragmentation; (2) HERWIG with coherent parton shower and cluster fragmentation; (3) ARIADNE with colour dipole model and string fragmentation; (4) COJETS with incoherent parton shower and independent fragmentation. All the parton shower models describe LEP2 data well.

Figure 2 shows comparisons of energy evolution of different event shape variables from L3 [3] with QCD model predictions. The energy dependence arise due to (a) logarithmic dependence of α_s on energy; and (b) fragmentation having a $1/Q^n$ dependence. As can be seen from the figure, all models with parton shower describe energy dependence well. Matrix element model uses calculations up to $\mathcal{O}(\alpha_s^2)$ and there the number of partons is too few. This is compensated by retuning at each centre of mass energy. So one does not expect the matrix element approach with one point tuning to explain energy evolution.

2.3 *Power correction*

The energy dependence of moments of the event shape variables can be described as a sum of the perturbative contribution and a power law dependence due to non-perturbative contribution [4]. For example, the first moment of an event shape variable f can be written as

$$\langle f \rangle = \langle f_{\rm pert} \rangle \ + \ \langle f_{\rm pow} \rangle,$$

where the perturbative contribution $\langle f_{\rm pert} \rangle$ can be expressed at $\mathcal{O}(\alpha_s^2)$ as:

$$\langle f_{\rm pert} \rangle = A \frac{\alpha_s(Q)}{2\pi} \ + \ (B + A \cdot (\beta_0 \ln \mu - 2)) \left(\frac{\alpha_s(Q)}{2\pi} \right)^2,$$

with A and B being known numbers obtained using ERT matrix elements, μ is related to the renormalization scale ($= Q/\sqrt{s}$) and β_0 = $(11 \cdot N_c - 2N_f)/3$. The power correction term is given by

$$\langle f_{\rm pow} \rangle = c_f \cdot \mathcal{P},$$

where the term c_f depends on the type of event shape variable f. $\mathcal{P}$ is supposed to have a universal form:

$$\mathcal{P} = \frac{4C_F}{\pi^2} \mathcal{M} \frac{\mu_I}{\sqrt{s}} \left[\alpha_0(\mu_I) - \alpha_s(\sqrt{s}) - \beta_0 \frac{\alpha_s^2(\sqrt{s})}{2\pi} \left(\ln \frac{\sqrt{s}}{\mu_I} + \frac{K}{\beta_0} + 1 \right) \right],$$

where α_0 is a non-perturbative parameter accounting for contributions to the event shape below an infrared matching scale μ_I (= 2 GeV), K = (67/18 $-$ π^2/6)$\cdot C_A - 5N_f/9$. The Milan factor $\mathcal{M}$ is 1.49 for N_f = 3. For the jet broadening variables, there is an additional shift which can be described as an additional multiplicative factor F to $\mathcal{P}$:

$$F = \left(\frac{\pi}{2\sqrt{a \cdot C_F \alpha_{\rm CMW}}} + \frac{3}{4} - \frac{\beta_0}{6a\, C_F} + \eta_0 + \mathcal{O}(\sqrt{\alpha_s}) \right),$$

where η_0 is -0.6137, a = 1 (2) for B_T (B_W) and $\alpha_{\rm CMW}$, defined as

$$\alpha_{\rm CMW} = \alpha_s \left(1 + K \frac{\alpha_s}{2\pi} \right)$$

is determined at $\sqrt{s} \cdot {\rm e}^{-3/4}$.

L3 has carried out fits to the first moments of the five event shape variables. α_0 and α_s are the only free parameters in the fit. The renormalization scale is fixed at $Q = \sqrt{s}$. The results of the fits are shown in figure 3. The four values of α_0 obtained from the four event shape variables ρ, B_T, B_W and C agree well within errors. The value obtained from $1-T$ is within $2 \cdot \sigma$ from the other four values. These measurements are in reasonable agreement with the predicted universality of the power law behaviour. The five estimates of α_0 can be combined to get an overall α_0 of 0.537 $\pm$ 0.069.

L3 has also analysed the second moments in terms of power law corrections. For variables $1-T$, ρ and C, the following result is expected to hold

$$\langle f^2 \rangle = \langle f_{\rm pert}^2 \rangle \ + \ 2 \langle f_{\rm pert} \rangle \cdot c_f \mathcal{P} \ + \ \mathcal{O}\left(\frac{1}{Q^2} \right).$$

This assumes that the non-perturbative correction to the distributions just cause a shift. For jet broadenings the power corrections are not just a shift and the formula would be more complicated. One uses fit results from first moments for the first two terms ($\alpha_s(m_Z)$, α_0(2 GeV)).The remaining term $\left(A_2/Q^2\right)$ is obtained from a fit for each variable. A_2 is supposed to be small, but has been found substantial for $1-T$, B_T, C.

2.4 α_s

DELPHI [5] examined 18 event shape variables using 1.5 million hadronic Z decays from LEP. They fitted the measured distributions to $\mathcal{O}(\alpha_s^2)$ calculations in a range where theory can describe data. Oriented distributions $R(y, \cos\theta_T)$ for several variables y were fitted with $|\cos\theta_T| < 0.84$.

If the scale μ was fixed to 1, the fit quality was poor and α_s values were scattered over a large region: $\alpha_s(m_Z)$ = 0.1228 $\pm$ 0.0119. On the other hand, if fits were performed with α_s as well as μ as parameters, good fits (χ^2/d.o.f. $\approx$ 1) were obtained and the scatter in α_s values was considerably reduced: $\alpha_s(m_Z)$ = 0.1167 $\pm$ 0.0026. But μ varied from 0.0033 ($1-T$) to 7.10 (D_2^{Geneva}).

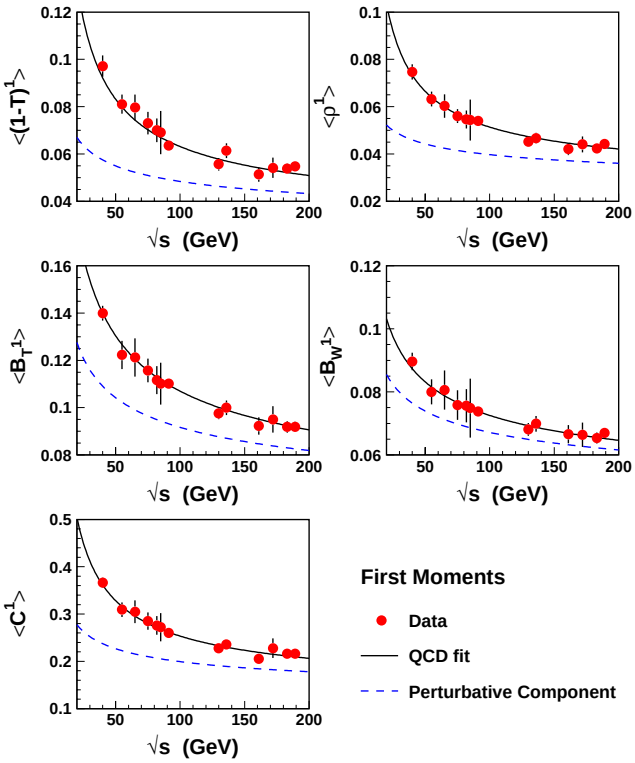

Figure 3. First moments of the event shape variables, $1-T$, ρ, B_T, B_W, C as measured by L3 as a function of centre of mass energy with fits to QCD predictions.

The standard approach to determine α_s from event shape distributions is to combine fixed order calculations with resummed leading and next-to-leading log calculations. Analytical calculations exist up to $\mathcal{O}(\alpha_s^2)$:

$$R(\alpha_s, y) \equiv \int_0^y \frac{1}{\sigma}\frac{\mathrm{d}\sigma}{\mathrm{d}y} = \left(\frac{\alpha_s}{2\pi}\right)\cdot A(y) \; + \; \left(\frac{\alpha_s}{2\pi}\right)^2 \cdot [B(y) \; + \; 4\pi\beta_0 \; \ln\mu \; A(y)]$$

for event shape variable $y(1-T, \rho, B_T, B_W, C)$, where A, B are obtained using ERT matrix elements. These calculations describe data well in multi-jet region (large y), but fail in the two jet region (small y) where multiple soft/collinear gluon emissions become dominant.

Resummed (to all orders) calculations of leading log ($L \sum (\alpha_s L)^n$ with $L \equiv (\ln \; 1/y)$) and next-to-leading log ($\sum(\alpha_s L)^n$) terms exist for certain variables. These calculations describe data well at small y values. So if one combines the two calculations taking care of common terms and fulfilling kinematic constraints at $y = y_{\max}$, one expects to describe data well over a wide kinematic region. Hadronization effects are folded in using parton shower Monte Carlo. These corrections are small at high energies ($\sim$ 10% at $\sqrt{s} \simeq m_Z$).

The four experiments [1–3,6] use different fit ranges. In particular, L3 uses wider fit range, probing small y values. Good fits are obtained for all the variables over a wide range of centre of mass energies by each of these experiments. The measurements from the 4 LEP experiments and at different centre of mass energies have been combined in figure 4. All the measurements are consistent with $\alpha_s(m_Z) = 0.122 \pm 0.004$. One should note that the four experiments use different sets of variables in this α_s determination. Parameter sets for ALEPH, DELPHI, L3 and OPAL are respectively (T, $-\ln y_3$, m_H, B_W, C), (T, ρ), (T, ρ, B_T, B_W, C) and (T, y_3, ρ, B_T, B_W, C).

OPAL [7] examined 5 event shape variables (y_{23}, $1-T$, m_H, B_W, C) in 4.4 M hadronic Z decays to study flavour dependence in α_s. They classify the event sample by quark flavour (a) using secondary vertex tagging with the help of silicon vertex detector leading $\epsilon \sim 23$ %, $\Pi \sim 86$% for b events and $\epsilon \sim 35$ %, $\Pi \sim 96$% for u, d, s events; (b) using $D^\star$ events with a cut on $\Delta M = M_{D^*} - M_{D^0}$ which gives $\epsilon \sim 2$ %, $\Pi \sim 55$% for c events. OPAL fits tagged samples to combinations of uds, c, b components with $3\alpha_s$ taking care of quark mass effect. They obtain:

$$\alpha_s^c/\alpha_s^{uds} = 0.997 \pm 0.038 \pm 0.030 \pm 0.012,$$
$$\alpha_s^b/\alpha_s^{uds} = 0.993 \pm 0.008 \pm 0.006 \pm 0.011.$$

2.5 *Heavy flavour*

DELPHI [8] measured 3- and 4-jet rates in hadronic Z decays with quark flavour tagged as b-quark or light (u, d, s) quark. Two different tagging methods were used utilizing (a) signed impact parameter; (b) multiple characteristic variables giving 85% pure uds or b quark events. ALEPH [9] used flavour tagging in jet rates or event shape variables. Gluon branching rate depends on quark mass and this dependence has been used in extracting b-mass at a scale of m_Z. The measurements are summarized in table 1.

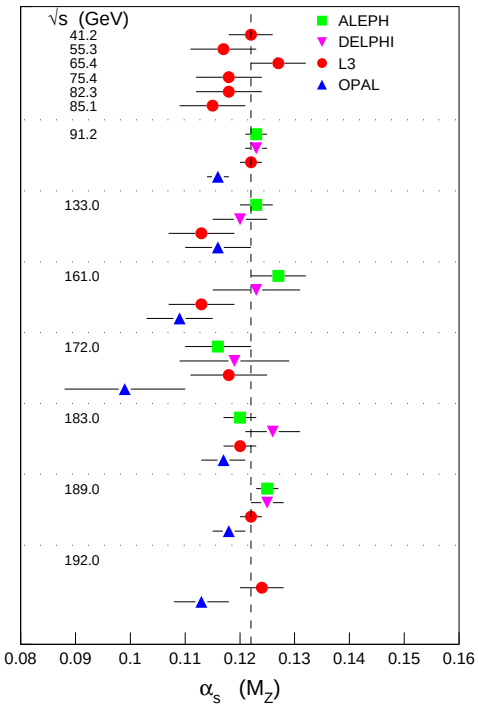

Figure 4. α_s measurements by the 4 LEP experiments from global event shape variables at different centre of mass energies run to $Q = m_Z$.

Table 1. b-quark mass measured at a scale of m_Z from gluon branching rate.

	$m_b(m_Z)$ (GeV)	Δm_b (GeV)			
		Stat.	Syst.	Had.	Theory
ALEPH	3.78	0.14	0.17	0.10	$^{+0.12}_{-0.13}$
DELPHI	2.61	0.18	0.04	$^{+0.45}_{-0.49}$	0.07
SLD	2.52	0.27		$^{+0.33}_{-0.47}$	$^{+0.54}_{-1.46}$

These results should be compared with $m_b(m_Z) = 4.20 \pm 0.08$ GeV from QCD sum rule and NNLO in $\Upsilon(1S)$. One sees the running of quark mass as expected from QCD.

The LEP experiments continue flavour tagging [10] in hadronic data at LEP2. L3 and DELPHI use vertex tagging to obtain R_b and R_{uds}. Figure 5 shows the measurements from DELPHI at LEP2 energies. The electroweak theory explain the data at all these energies.

Uncertainty in the determination of gluon splitting probability to heavy flavour constitutes the largest systematics in R_b and R_c determinations. Measurements from Z data before 1999 can be summarized as:

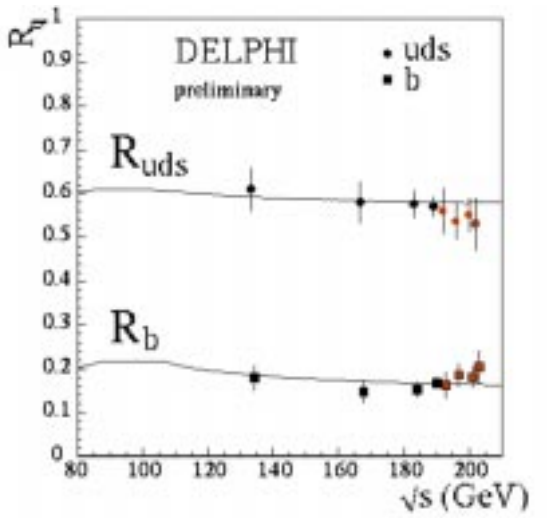

Figure 5. Ratio of flavour tagged to total hadronic cross-section as a function of centre of mass energy compared with predictions from electroweak theory.

Table 2. Gluon splitting probability measured by the LEP experiments.

L3	$n_{g\to c\bar{c}}$	$\left[2.45 \pm 0.35 \pm 0.45 - 3.74(n_{g\to b\bar{b}} - 0.26)\right]\%$
OPAL	$n_{g\to c\bar{c}}$	$[3.20 \pm 0.21 \pm 0.38]\ \%$
	$n_{g\to b\bar{b}}$	$[0.215 \pm 0.043 \pm 0.080]\ \%$
DELPHI	$n_{g\to b\bar{b}}$	$[0.33 \pm 0.10 \pm 0.08]\ \%$

$$n_{g\to c\bar{c}} = 2.2\%,$$
$$n_{g\to b\bar{b}} = 0.2\%.$$

Recent measurements exist from L3, DELPHI and OPAL [11]. L3 looked at 3-jet events. They identified c-quarks in the gluon jet (a) from a study of leptons in the least energetic jet, (b) by carrying out a neural network analysis with energy flow variables. They obtained $\epsilon_c = 0.4$–4.4% and $\epsilon_b = 1$–13%. OPAL made an analysis of 4-jet events and DELPHI studied 4-b events. The results are summarized in table 2.

ALEPH and L3 [12] looked for the process $e^+e^- \to t\bar{c}\ (\bar{u})$; $t \to bW$ and $W \to f\bar{f}'$. Standard Model expects a cross-section $\leq 10^{-9}$ pb for such a process. The search strategy relied on the facts that top is almost at rest (near threshold) and accompanying light quark will have little energy. So b, W from top decay will be almost monochromatic and Wb system will cluster around top mass. W can decay to leptons (missing energy) or to jets ($\ell\nu$, $q\bar{q}'$ cluster around m_W).

L3 examined data at $\sqrt{s}$ = 183 GeV and observed 0(1) events in the $\ell\nu$ $(q\bar{q}')$ channel where background from Standard Model processes is expected to be 0.3 (3.8). They quoted 95% CL upper limit for cross section of the FCNC process of 575 pb (1610 pb).

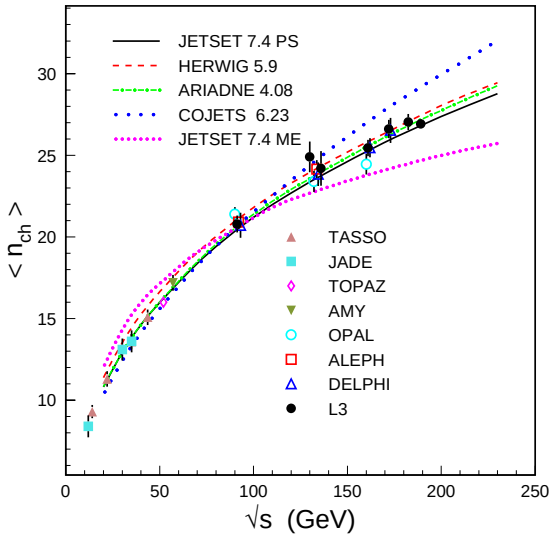

Figure 6. Energy evolution of mean charged particle multiplicity compared with predictions from different QCD models.

From the data at $\sqrt{s}$ = 189 GeV, ALEPH observed 2 (16) events in the $\ell\nu$ $(q\bar{q}')$ channel where background expectation was 1(10.5). The small excess in the data has not been confirmed with their 1999 data sample where 30 events have been observed with 26.3 events expected from background.

2.6 *Inclusive spectra*

Figure 6 shows measurements of mean charged particle multiplicity as a function of centre of mass energy. The data are compared with predictions of various QCD models. Coherent parton shower models with soft gluon suppression explains energy evolution of $\langle n_{ch} \rangle$. COJETS with incoherent parton shower predicts too high multiplicity at high $\sqrt{s}$ values.

Soft gluon coherence depletes particles at low x_p $(\equiv 2p/\sqrt{s})$ values. This gives rise to bell like structure in ξ_p $(\equiv \ln(1/x_p))$. The ξ_p distribution takes a Gaussian form asymptotically. But in MLLA, it can be represented by a skewed Gaussian. Data from different LEP experiments at various centre of mass energies have been fitted to the skewed Gaussian distribution. The peak positions in the ξ_p distributions ($\xi^\star$) increase with $\sqrt{s}$ and QCD together with LPHD (local hadron parton duality) hypothesis predict a specific energy dependence of $\xi^\star$. The leading log approximation (DLA) gives a poor description of the energy evolution, whereas MLLA calculation with $\Lambda_{\rm eff} \approx 200$ MeV describe data well.

2.7 *BE correlation and colour reconnection*

Bose–Einstein correlation between like sign pions has been observed in Z and W decays at LEP. There have been considerable studies to examine if such correlations exist among decay products of two W's. Such final state interaction effect will influence determination of m_W. ALEPH [13] has compared like sign to unlike sign particle pair distribution in the

process $e^+e^- \rightarrow W^+W^-$. BE correlation observed in $q\bar{q}'\ell\nu$ mode of W-production is well reproduced by MC tuned to BE correlation data at LEP1. There is a better agreement between data and MC with BE correlation implemented only for π's of the same W. Models with correlation also among π's of different W's have been found to be disfavoured at 2.7σ level.

For the process $e^+e^- \rightarrow W^+W^-$, $W^+ \rightarrow q_1\bar{q}_2$, $W^- \rightarrow q_3\bar{q}_4$, each quark pair will hadronize independently in absence of cross talk. QCD interference causes gluon exchange between 2 initial $q\bar{q}'$. This will result a change in particle distributions. Comparison of multiplicities in $q\bar{q}'\ell\nu$ and 4-quark final states does not show any appreciable difference. However, this method is not sensitive enough to discriminate colour reconnection.

Recently, L3 [14] has examined energy and particle flow in inter-jet region. One expects, even with colour reconnection, the jets to correspond to initial quark direction. One uses topological criteria to order the jets and select 4-jet sample where the association of jets to the W's is unique. In these events, a plane is defined by two jets, particle momenta are then projected in this plane and the directions of the particles are defined by the angle ϕ with respect to a reference direction. Figure 7 shows energy and particle flow as a function of ϕ.

To compare different inter-jet region, the angle ϕ is rescaled with respect to angle between jets. Since W-pair events are not coplanar, it is better to use 4 planes rather than 1 defined by adjacent jets and the appropriate plane is chosen for a given particle. Particle density or energy flow between q's from the same W are expected to be different from those from different W's. So if one examines ratios in the two regions, one expects sizable differences ($\sim$ 10%) among some of the reconnection models. Data are not yet sensitive to discriminate models. But one expects to rule out some of the models with final statistics of LEP data. Asymmetries in energy, particle flow are also found to be suitable for such studies.

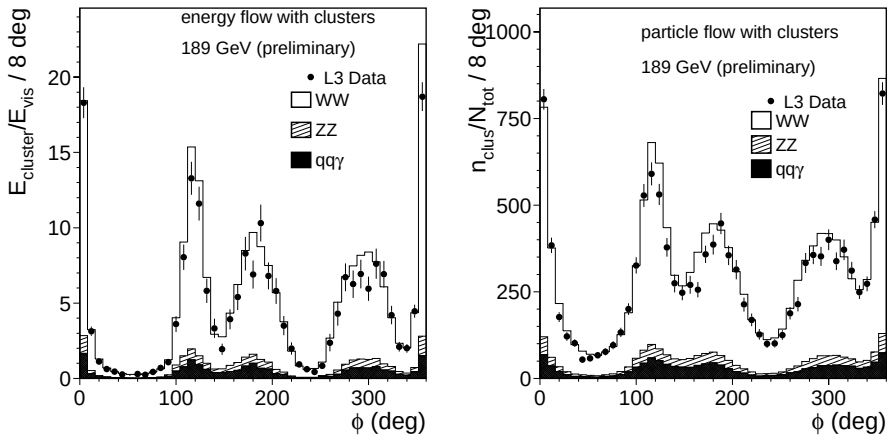

Figure 7. Energy and particle flow in the 4-jet sample at $\sqrt{s}$ = 189 GeV compared to predictions of Standard Model.

3. 2-Photon processes

Here, one studies associated hadron production with scattered electron and positron. Depending on detection of scattered $e^{\pm}$, one can look at (a) untagged events (where both the photons are almost on shell); (b) single tag events (with one real and one highly virtual photon); (c) double tag events (where both the photons are highly virtual). Recent measurements exist on $\gamma\gamma$ total cross section, inclusive c and b production and jet production in the untagged sample; on photon structure function in the single tag sample and on $\gamma^{\star}\gamma^{\star}$ cross section in the double tag sample.

3.1 $\gamma\gamma$ *Total cross-section*

The visible centre of mass energy of the hadronic system $(W_{\rm vis})$ is always smaller than the true centre of mass energy $(W_{\gamma\gamma})$ and one has to use unfolding methods with Monte Carlo samples to convert measured $W_{\rm vis}$ to $W_{\gamma\gamma}$. This unfolding depends critically on the Monte Carlo model used and one finds the two models PHOJET and PYTHIA agree at 20–30% level.

L3 and OPAL [15] used unfolded $W_{\gamma\gamma}$ to determine experimentally measured cross-section $\sigma(e^+e^- \rightarrow e^+e^- + \text{hadrons})$ and observed that σ_{eeh} increases with increasing $\mathrm{E_{beam}}$ and decreasing $W_{\gamma\gamma}$. The effect of $\gamma\gamma$ luminosity has been taken out using

$$\frac{\mathrm{d}\sigma_{eeh}}{\mathrm{d}(W^2_{\gamma\gamma}/s)} = \int \frac{\mathrm{d}Q^2}{Q^2}\frac{\mathrm{d}P^2}{P^2} \sum_{a,b=T,S} \mathcal{L}_{ab}\sigma^{\gamma\gamma}_{ab}(W_{\gamma\gamma}, P^2, Q^2)$$

$$\sigma^{\gamma\gamma}_{ab}(W_{\gamma\gamma}, P^2, Q^2) = F_a(Q^2)F_b(P^2)\sigma^{\gamma\gamma}_{ab}(W_{\gamma\gamma}),$$

where the summation is over all photon helicity states. One can then extract $\sigma^{\gamma\gamma}$ taking care of γ form factors.

Figure 8 shows the measurements of cross-section using two different generators for energy unfolding. The measurements from L3 and OPAL are compatible if the same generator is used in unfolding but there is significant difference between the two generators PHOJET and PYTHIA. Both the experiments show clear rising cross-section with energy. At high $W_{\gamma\gamma}$, Pomeron exchange dominates and one expects an energy dependence [16]:

$$\sigma_{\rm tot} = A \cdot s^{\epsilon} + B \cdot s^{-\eta}.$$

Fixing η = 0.34 (as obtained from a fit to all hadronic $\sigma_{\rm tot}$), one gets ϵ value of 0.22 ± 0.02, which is 7σ different from the universal fit ($\epsilon = 0.095 \pm 0.002$). This indicates a contribution of an additional Pomeron term with $\alpha_{\rm soft}(0) \sim 1.08$ and $\alpha_{\rm hard}(0) \sim 1.4$. Other approaches like (a) smooth suppression of hadron-like and point-like γ interaction, (b) dual parton model with unitarization constraint, (c) mini-jet model using QCD to calculate number of hard collisions, can also explain this behaviour.

3.2 *Heavy flavour production*

Cross-section for heavy flavour production in $\gamma\gamma$ processes are calculable in perturbative QCD. Measurements exist for charm pair production [17] from ALEPH (using $D^{\star\pm}$ tag),

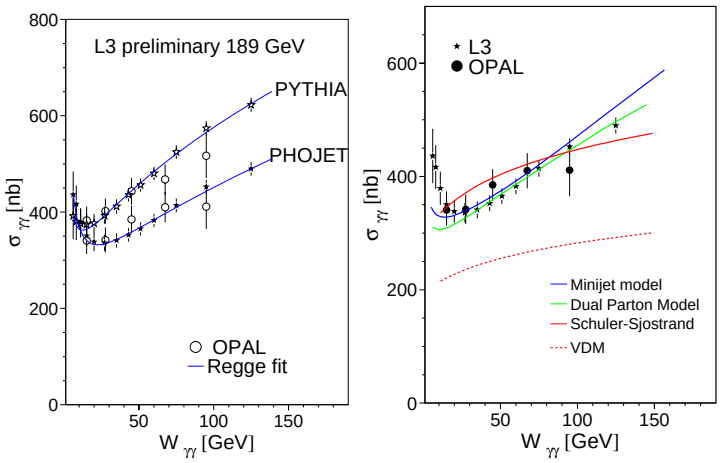

Figure 8. Measured $\sigma^{\gamma\gamma}$ as a function of centre of mass energy compared to various models.

L3 (using $D^{\star\pm}$ and high $p_\perp$ lepton tag) and OPAL (using $D^{\star\pm}$ tag). L3 also quotes the first measurement of $b\bar{b}$ production:

$$\sigma_{b\bar{b}} \;=\; 9.9 \;\pm\; 2.9\,(stat) \;\pm\; 3.8\,(syst)\; pb.$$

One finds $\sigma(e^+e^- \to e^+e^- c\bar{c} + X)$ increases with $\sqrt{s}$ and the direct process is insufficient to describe data. Thus, it provides evidence of gluon component in photon. Differential distributions $(p_\perp^{D^*}/W_{\rm vis}, x_\gamma, \ldots)$ have better discrimination between direct and resolved process and these distributions have been used by OPAL to demonstrate inadequacy of direct process alone.

3.3 *Di-jet production*

OPAL [18] has studied jet production in 2-photon process. They separate direct and resolved processes in two jet sample using

$$x_\gamma^{\pm} = \frac{\sum_{\rm jet}(E \pm p_z)}{\sum_{\rm had}(E \pm p_z)}.$$

The direct process due to quark exchange ($x_\gamma^{\pm} < 0.8$) is well separated from the resolved process due to gluon exchange ($x_\gamma^{\pm} > 0.8$). The measurements of jet angular distributions of these two components agree well with NLO QCD calculations.

3.4 γ *Structure function*

The four LEP experiments [19] use single tag data to measure photon structure function over a wide kinematic region. One expects quark constituents to be dominant at large x

and gluon constituents to be dominant at small x. Data from the 4 experiments cover Q^2 from 1 to 3000 GeV^2 and x down to 0.001, as can be seen from table 3.

One needs unfolding to take care of $W_{\rm vis} \to W_{\gamma\gamma}$ and the effect of virtuality of the photon. Good agreement is observed among the four experiments, but there is a need for better MC's. At the low Q^2 region, one finds the SAS-1d model [20] with evolution starting at Q_0^2 = 0.36 GeV^2 lying below data and the GRV model [21] with evolution starting at Q_0^2 = 0.25 GeV^2 can describe the low x region better. At medium Q^2, difference among models are small and data are in agreement with models. At high Q^2, quark parton model is found to be insufficient to describe data below $x < 0.3$, whereas the leading order calculations of GRV model and those of SAS-1d model agree well with data.

Figure 9 shows F_2^γ measured at 3 different x regions as a function of Q^2. One finds the $\ln Q^2$ evolution of F_2^γ to be well established. At high x region, all QCD models agree among themselves and with data. At low x, these models diverge and a better agreement with data is required.

3.5 $\gamma^\star\gamma^\star$

In double tag events, both γ's are virtual. BFKL diagram [22] is predicted to be dominant in $\gamma^\star\gamma^\star$ collision for $y = \ln\left(W^2_{\gamma^\star\gamma^\star}/\sqrt{Q^2P^2}\right) >> 1$. In leading order approximation

$$\begin{aligned}\sigma_{\gamma^\star\gamma^\star} &= \sigma_0\left(Q^2, Y\right)\left(\frac{s}{s_0}\right)^{\alpha_P - 1} \\ &= \sigma_0\left(Q^2, Y\right)\,\exp\left[Y\cdot(\alpha_P - 1)\right]\end{aligned}$$

with $\alpha_P - 1 = 4\ln(2N_c\alpha_s/\pi)$. Using $N_c = 3$, $\alpha_s = 0.2$, one expects $\alpha_P - 1 \approx 0.53$. Next to leading order calculations give $\alpha_P - 1 \leq 0.175$.

Table 3. Kinematic region of data used by the 4 LEP experiments to study γ structure function.

	$\sqrt{s}$ (GeV)	$\theta_{\rm Tag}$ (mrad)	Q^2 (GeV^2)	x
ALEPH	91	65–150	6–44	0.005–0.90
	91	318–927	35–3000	0.03–0.97
	183	35–155	7–200	0.003–0.97
DELPHI	91	43–135	4–30	0.005–0.977
	161, . . . , 189	42–610	10–1000	0.01–0.8
L3	91	26–66	1.2–9	0.002–0.2
	91	200–600	40–500	0.05–0.98
	183	30–66	9–30	0.01–0.3
OPAL	91	27–55	1.1–6.6	0.0025–0.2
	161, 172	33–120	6–100	0.02–0.6
	91, 189	25–60	1.5–30	0.001–0.32

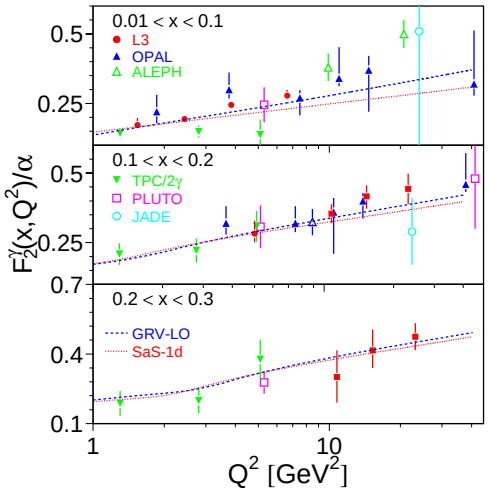

Figure 9. Q^2 evolution of F_2^γ measured at 3 different x regions compared to model calculations.

L3 and OPAL [23] reported measurements of $\gamma^\star\gamma^\star$ cross-sections. OPAL had 44 events from 189 GeV data with $\langle Q^2\rangle$ = 17 GeV^2 for $2 < Y < 6$, $E_e > 33$ GeV, $34 < \theta_e < 55$ mrad, $W_{\gamma\gamma} > 5$ GeV. L3 reported 37, 34, 108 events from their 91, 183 and 189 GeV data corresponding to $\langle Q^2\rangle$ of 3.5, 14 and 14.5 GeV^2 respectively. The measured cross-sections and Y distributions demonstrate that (a) direct process is insufficient to explain the data, (b) Monte Carlo predictions of TWOGAM and PHOJET agree well with the data at large Q^2, (c) the measured cross section requires $\alpha_P - 1$ which is smaller than expectation from leading order BFKL calculation but larger than NLO calculation. The χ^2/d.o.f. for the two fits are 263/10 and 21/10 for LO and NLO calculations respectively.

4. Summary

e^+e^- annihilation data to hadrons in the high energy LEP runs have given rise to many tests to QCD

- QCD models which include soft gluon coherence effects are in good agreement with the data.
- The accuracy in the extraction of α_s is reaching its limits. All α_s values extracted from event shape distributions are consistent with $\alpha_s(m_Z)$ = 0.122 $\pm$ 0.004.
- Substantial progress has been made in understanding the power correction to the perturbative component for event shape variables. This could eventually lead to a precise determination of α_s.
- LEP data has been used in measuring running mass of heavy quark, gluon splitting probabilities, ...
- One begins to understand QCD effects in W-mass measurement.

LEP is providing excellent results in the field of 2-photon physics

- Evidence of gluon component in photon is observed.
- QCD is being tested in the hadronic photon structure function.
- BFKL is inadequate in explaining $\gamma^\star\gamma^\star$ cross-section.

One requires more theoretical works to match good precision of the data.

Acknowledgements

I would like to thank all the LEP colleagues for their contribution. I am grateful to M N Kienzle-Focacci and M Wadhwa for encouraging discussions. I would thank the warm hospitality of WHEPP-6 organisers.

References

[1] DELPHI Collab: J Drees *et al*, EPS, Tampere, 1999
[2] OPAL Collab: G Abbiendi *et al*, CERN-EP/99-175
[3] L3 Collab: M Acciarri *et al*, Winter Conferences 2000, L3 Note # 2504
[4] Yu L Dokshitzer and B R Webber, *Phys. Lett.* **B352**, 451 (1995)
B R Webber, hep-ph-9510283
Yu L Dokshitzer *et al*, *Nucl. Phys.* **B511**, 396 (1997)
Yu L Dokshitzer *et al*, *Journal of High Energy Physics* **05**, 3 (1998)
Yu L Dokshitzer *et al*, hep-ph-9812487
Yu L Dokshitzer, hep-ph-9911299
[5] DELPHI Collab: P Abreu *et al*, CERN-EP/99-133
[6] ALEPH Collab: G Dissertori *et al*, EPS, Tampere, 1999, ALEPH 99-023
[7] OPAL Collab: G Abbiendi *et al*, *Europhys. J.* **C11**, 643 (1999)
[8] DELPHI Collab: S Cabrera *et al*, EPS, Tampere, 1999
[9] ALEPH Collab: G Dissertori *et al*, EPS, Tampere, 1999, ALEPH 99-059
[10] DELPHI Collab: P Abreu *et al*, EPS, Tampere, 1999
L3 Collab: M Acciarri *et al*, EPS, Tampere, 1999
[11] DELPHI Collab: P Abreu *et al*, *Phys. Lett.* **B462**, 425 (1999)
L3 Collab: M Acciarri *et al*, CERN-EP/99-156
OPAL Collab: G Abbiendi *et al*, CERN-EP/99-089
[12] ALEPH Collab: R Barate *et al*, EPS, Tampere, 1999 LEPC, November 1999
L3 Collab: M Acciarri *et al*, EPS, Tampere, 1999
[13] ALEPH Collab: R Barate *et al*, CERN-EP/99-173
[14] L3 Collab: M Acciarri *et al*, Winter Conferences 2000, L3 Note # 2503
[15] L3 Collab: M Acciarri *et al*, *Phys. Lett.* **B408**, 450 (1997); EPS, Tampere, 1999
OPAL Collab: G Abbiendi *et al*, CERN-EP/99-076
[16] A Donnachie *et al*, *Phys. Lett.* **B296**, 227 (1992)
[17] L3 Collab: M Acciarri *et al*, EPS, Tampere, 1999
OPAL Collab: G Abbiendi *et al*, EPS, Tampere, 1999
[18] OPAL Collab: K Ackerstaff *et al*, *Z. Phys.* **C73**, 433 (1997)
OPAL Collab: G Abbiendi *et al*, *Europhys. J.* **C6**, 253 (1999)
[19] ALEPH Collab: R Barate *et al*, *Phys. Lett.* **B458**, 152 (1999)
DELPHI Collab: *Workshop on Photon Interactions and the Photon Structure* , Lund, 1998
L3 Collab: M Acciarri *et al*, *Phys. Lett.* **B436**, 403 (1998); *Phys. Lett.* **B447**, 147 (1999)

OPAL Collab: K Ackerstaff *et al*, *Z. Phys.* **C74**, 33 (1997); *Phys. Lett.* **B411**, 387 (1997); *Phys. Lett.* **B412**, 325 (1997); EPS, Tampere, 1999
[20] G A Schuler *et al*, *Z. Phys.* **C68**, 607 (1995); *Phys. Lett.* **B376**, 193 (1996)
[21] M Glück *et al*, *Phys. Rev.* **D45**, 3986 (1992); *Phys. Rev.* **D46**, 1973 (1992)
[22] E A Kuraev *et al*, *Sov. Phys. JETP* **45**, 199 (1977)
Ya Ya Balitski *et al*, *Sov. J. Nucl. Phys.* **28**, 822 (1978)
[23] L3 Collab: M Acciarri *et al*, *Phys. Lett.* **B453**, 333 (1999); EPS, Tampere, 1999
OPAL Collab: G Abbiendi *et al*, EPS, Tampere, 1999